

Plasmonic Biosensors Based on Deformed Graphene

Vahid Faramarzi ¹, Mohsen Heidari ¹, Nik Humaidi bin Nik Zulkarnine ² and Michael Taeyoung Hwang ^{3,*}¹ Department of Electrical and Computer Engineering, Tarbiat Modares University, Tehran 14115-194, Iran² Department of Chemistry, Faculty of Science, University Malaya, Kuala Lumpur 50603, Malaysia³ Department of BioNano Technology, Gachon University, 1342 Seongnamdae-ro, Sujeong-gu, Seongnam 13120, Gyeonggi, Republic of Korea

* Correspondence: anol81@gachon.ac.kr

Abstract: Rapid, accurate, and label-free detection of biomolecules and chemical substances remains a challenge in healthcare. Optical biosensors have been considered as biomedical diagnostic tools required in numerous areas including the detection of viruses, food monitoring, diagnosing pollutants in the environment, global personalized medicine, and molecular diagnostics. In particular, the broadly emerging and promising technique of surface plasmon resonance has established to provide real-time and label-free detection when used in biosensing applications in a highly sensitive, specific, and cost-effective manner with small footprint platform. In this study we propose a novel plasmonic biosensor based on biaxially crumpled graphene structures, wherein plasmon resonances in graphene are utilized to detect variations in the refractive index of the sample medium. Shifts in the resonance wavelength of the plasmon modes for a given change in the RI of the surrounding analyte are calculated by investigating the optical response of crumpled graphene structures on different substrates using theoretical computations based on the finite element method combined with the semiclassical Drude model. The results reveal a high sensitivity of 4990 nm/RIU, corresponding to a large figure-of-merit of 20 for biaxially crumpled graphene structures on polystyrene substrates. We demonstrate that biaxially crumpled graphene exhibits superior sensing performance compared with a uniaxial structure. According to the results, crumpled graphene structures on a titanium oxide substrate can improve the sensor sensitivity by avoiding the damping effects of polydimethylsiloxane substrates. The enhanced sensitivity and broadband mechanical tunability of the biaxially crumpled graphene render it a promising platform for biosensing applications.

Keywords: crumpled graphene; plasmonic resonance; refractive index; absorbance; mid-infrared



Citation: Faramarzi, V.; Heidari, M.; Zulkarnine, N.H.b.N.; Hwang, M.T. Plasmonic Biosensors Based on Deformed Graphene. *Biophysica* **2022**, *2*, 538–547. <https://doi.org/10.3390/biophysica2040045>

Academic Editor: Danilo Milardi

Received: 21 October 2022

Accepted: 23 November 2022

Published: 29 November 2022

Publisher's Note: MDPI stays neutral with regard to jurisdictional claims in published maps and institutional affiliations.



Copyright: © 2022 by the authors. Licensee MDPI, Basel, Switzerland. This article is an open access article distributed under the terms and conditions of the Creative Commons Attribution (CC BY) license (<https://creativecommons.org/licenses/by/4.0/>).

1. Introduction

Refractive index (RI) sensing is of significant interest for real-time biosensing applications, such as food safety, environmental monitoring, and medical diagnosis, particularly in the mid-infrared (mid-IR) range [1–6]. This is because other parameters such as the concentration, density, and stress can be detected by measuring the RI to identify a particular substance. The specific antigen–antibody binding and chemical or biochemical interactions are monitored directly by observing a RI change, which needs no label. In particular, RI sensing are becoming a widespread medical diagnosis technique to detect and monitor cancerous tumors through the detection of different biomarkers such as circulating tumor cells [7]. Since the cancer biomarkers are present in bodily fluids such as blood, such detection could enable liquid biopsy, which can replace invasive tumor-tissue biopsies in many diagnostic applications and make them less painful and also reduce the chances of infections. Therefore, the presence of biomarkers induces a considerable change in sample RI demonstrating the important role of RI sensing in detecting and monitoring cancer in the early stage [8,9].

Plasmonic-based RI sensors are widely used because of their compact size, high sensitivity, real-time detection, fast response, and lack of labeling requirements [10]. Surface

plasmon waves are highly sensitive to the RI of the medium on the sensor surface. Slight variations in the RI of the surrounding medium lead to a distinct shift in the resonant wavelength in the mid-IR range (~2.5–25 μm wavelength). Therefore, by monitoring this change, the presence of chemical and biological species near the sensor surface can be detected in real time. Recently, various types of surface plasmon resonance (SPR)-based RI sensors that rely on noble metals (e.g., Au and Ag) have been developed with different configurations, such as plasmonic waveguides [11], metamaterials [12], Fano resonance structures [13], and gap-ring patterns [14]. However, noble metal structures exhibit large ohmic losses in the mid-IR range because of their large dielectric constant and low charge-carrier mobility; additionally, they have limitations in terms of tuning conductivity, and cannot adsorb biomolecules efficiently because of their inherent hydrophobicity [15].

To overcome these shortcomings, approaches using surface plasmons in graphene as an emergent platform for SPR-based biosensors have been reported [16–21]. Graphene plasmons (GPs) exhibit unprecedented spatial confinement of electromagnetic fields with extremely short wavelengths compared with incident photons, thus opening interesting pathways for the nanoscale manipulation of light and for developing integrated plasmonic biosensors over wide frequency ranges. In particular, the mid-IR range is suitable for biosensing as the vibrational absorption signals of biomolecules that distinguishes biological building blocks, such as proteins and nucleic acids, are located in this frequency range [22]. However, developing graphene-based plasmonic sensors that depend on coupling between GPs and free-space electromagnetic waves is still a challenge. This is because of the large momentum mismatch between the GPs and incident photons, which requires conventional optical coupling configurations, such as prisms, gratings, and waveguide couplers, to convert incident light into propagating GPs [23]. However, these couplers are massive, time-consuming, and costly to fabricate. In addition, patterned structures in graphene are not reconfigurable; thus, realizing the broadband tunability of GPs over the IR wavelength range is challenging.

Theoretically, strong plasmonic resonances with broadband tunability have been shown to be supported using mechanically reconfigurable deformed graphene in a periodic structure [24]. Recent studies have demonstrated that crumpled graphene field-effect transistors (gFETs) with millimeter-scale structures exhibit higher sensitivity in the electronic detection of biomolecules compared with conventional flat gFETs [25–27]. In a previous study, we proposed an SPR biosensor based on crumpled graphene structures [28]. Although the sensor exhibited superior sensing performance on silicon, the plasmon resonances of graphene, and thus the sensitivity, were affected by the large photoabsorption intensity of the polymer substrate.

In this study, we propose a new RI sensor based on plasmonic resonances in biaxially crumpled graphene structures. We investigated the wavelength shifts in the plasmonic resonances of crumpled graphene structures with respect to variations in the RI of the analyte medium atop the graphene surface. We evaluated the sensing performance of the proposed RI sensor in terms of sensitivity and figure-of-merit (FOM) and compared it with that of a uniaxially crumpled graphene-based plasmonic sensor. We demonstrated that the shift in the plasmonic resonance wavelength for a specific change in RI with biaxially textured graphene structures was larger than that achieved with uniaxially crumpled graphene structures or conventional flat graphene-based plasmonic devices.

2. Results

The plasmonic resonances of the crumpled graphene structures placed on different substrates have been investigated. Figure 1 illustrates the proposed structure, which consists of biaxially crumpled graphene on a stretchable polymer substrate. The system is illuminated by transverse magnetic (TM) polarized light propagating along the crumpling directions x and y in the direction normal to the structure (K_0) from the top. The structure is described by crumpling width (W) and height (H).

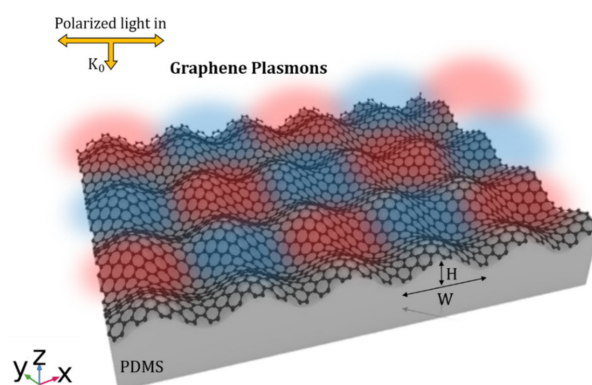


Figure 1. Schematic demonstration of a biaxially crumpled graphene structure with crumple width W and crumple height H . Polarized light with electric field E along the crumpling directions x and y illuminates in the normal direction K_0 to the structure.

To compare the sensitivity of biaxially crumpled graphene with that of uniaxially crumpled graphene, the plasmonic properties of devices composed of the two types of crumpled graphene on various substrates were studied. We investigated the absorption spectrum of the proposed structure under normal incidence to obtain plasmonic resonances in the proposed crumpled graphene structures. As shown in Figure 2, a higher number of plasmonic modes with larger absorption intensities and lower FWHM values (stronger plasmonic resonances) were observed for the free-standing biaxially crumpled graphene and the graphene supported on polystyrene (PS) and polydimethylsiloxane (PDMS) substrates as compared to the uniaxially crumpled graphene. For example, biaxially crumpled graphene supported on a PS substrate exhibited two plasmon resonances at wavelengths of approximately 7.8 and 5.8 μm , with absorption intensities of 0.4 and 0.34 and FWHM values of 144 and 48 nm, respectively (Figure 2b). However, for the uniaxially crumpled graphene structure on PS, one plasmon resonance appeared at approximately 7.8 μm , with an absorption intensity of 0.28 and FWHM of 79 nm (Figure 2e). The plasmon resonances of graphene can strongly overlap with the absorbance peaks of PDMS substrates in mid-infrared range. This results in damping, attenuating, and broadening of plasmon modes which negatively affect the sensing performance of the device. This problem can be addressed using biaxially crumpled graphene structure by having more plasmonic resonances which are largely detuned from destructive absorbance peaks of PDMS. Thus, distinct and sharp spectral resonances can be obtained by creating a large frequency detuning between the plasmon resonances and PDMS absorbance peaks using biaxial structure. The effect of the polymer substrate may not be easily excluded in practical sensing application, thus having two or more resonances which are largely detuned from the absorbance peaks of the substrate can improve the sensing performance of the device as these plasmon modes are sharp and isolated.

Thus, to achieve excellent sensing performance, high-quality plasmon resonance modes that possess higher absorption intensities and sharper frequency widths (lower FWHM values) are desirable as they enable the facile detection of the shift in resonance wavelengths caused by RI variations in the surrounding medium and biomolecules. In this regard, we investigated the effect of analyte solutions introduced into crumpled graphene-based RI sensors on plasmonic resonance wavelengths. Figure 3 compares the absorption spectra of biaxially and uniaxially crumpled graphene supported on PS and PDMS substrates as the RI of the sample medium varied (n_1) from 1.3 to 1.5. For the biaxially crumpled structure on the PS substrate, the plasmon resonance mode at 9.2 μm exhibited a wavelength shift of 998 nm as n_1 varied from 1.3 to 1.5 above the graphene surface. Whereas the shift for the uniaxially crumpled graphene was 870 nm at the same resonance wavelength. The shift in resonance wavelength of the plasmon mode at 10.5 μm for the biaxially and uniaxially crumpled graphene structures on the PDMS substrate was 530 and 414 nm, respectively. Subsequently, we compared biaxially and uniaxially crumpled graphene structures in terms of sensitivity and FOM. The biaxially crumpled structure on

PS substrate exhibited a sensitivity of 4990 nm/RIU and FOM of 20, whereas the uniaxial structure had a sensor sensitivity of 4350 nm/RIU and FOM of 43. For biaxially(uniaxially) crumpled graphene on PDMS, the sensitivity and FOM were 2650 nm/RIU (2073 nm/RIU) and 16 (10), respectively. The biaxially crumpled graphene on PDMS presented higher sensor sensitivity and FOM than the uniaxially one. Moreover, the overall sensor sensitivity and FOM for the biaxially crumpled graphene structures were higher than those obtained using flat graphene-based sensors [29–31].

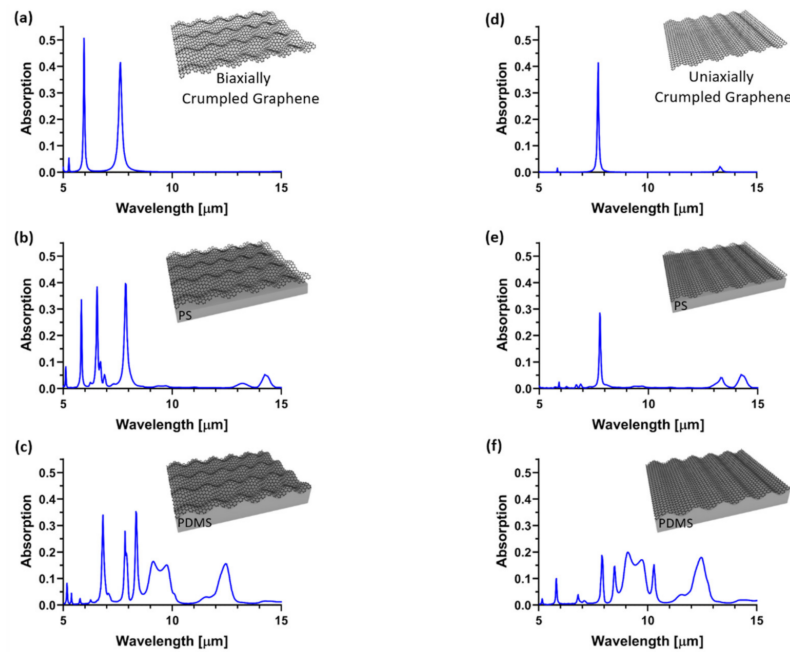


Figure 2. Optical absorption spectra of biaxially (a) free-standing crumpled graphene, supported on (b) flat PS and (c) corrugated PDMS substrates; and those of uniaxially (d) free-standing crumpled graphene, supported on (e) flat PS and (f) corrugated PDMS substrates. Here, $W = 250$ nm; $H = 300$ nm; and carrier mobility μ and Fermi energy level E_f are $10,000$ cm²/(V·s) and 0.64 eV, respectively.

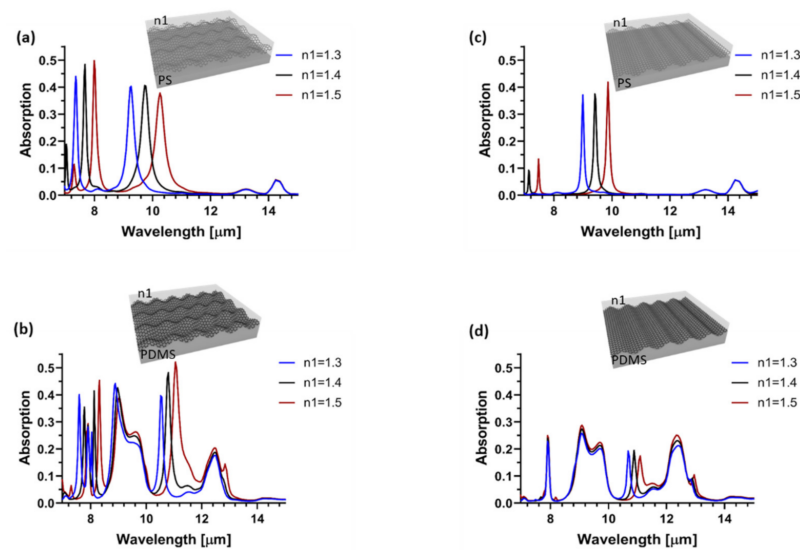


Figure 3. Plasmonic resonance shifts of biaxially crumpled graphene supported on (a) flat PS and (b) corrugated PDMS substrate; and those of uniaxially crumpled graphene on (c) flat PS and (d) corrugated PDMS substrate, when the RI of sample n_1 changed from 1.3 to 1.5, with geometrical parameters of $W = 250$ nm; $H = 300$ nm; $E_f = 0.64$ eV; and $\mu = 10,000$ cm²/(V·s).

The plasmon resonances in graphene are influenced by the damping effect of the substrate owing to the high absorbance of PDMS in the mid-infrared region. This results in a reduction in the wavelength shift of the graphene plasmon resonances and, thus, in the sensitivity of the device. Compared with the uniaxially crumpled structure, the plasmon resonances in the biaxially crumpled structures were less influenced by the damping effect of the substrate because the stronger plasmonic modes of the biaxially crumpled graphene enhanced the sensitivity and FOM of the sensor. In addition, when using biaxially crumpled structures, distinct plasmon resonances in the graphene detuned from the substrate absorbance peaks to avoid damping effects and improve the sensing performance of the device, in contrast to the strong coupling regime between the absorbance of the substrate and the plasmon resonances of graphene in the uniaxial structures.

Furthermore, the sensor sensitivity could be tuned using the mechanical reconfiguration of biaxially crumpled graphene structures. Figure 4 shows the wavelength shift of plasmonic resonances in biaxially crumpled graphene structures for various geometries with variable crumpled widths and heights when the RI of the medium on top of the graphene ranged from 1.3 to 1.5. The sensitivity of the sensor ranged from 2307 to 2975 nm/RIU for the structures presented in Figure 4; essentially, these values were higher than those obtained for the uniaxially crumpled structures with different geometries [28]. As shown in Figure 4, the broadband spectral tunability for the sensor can be obtained by mechanical reconfiguration of crumpled graphene structures. By tuning the structural parameters such as crumpled width and height, we can observe distinct and sharp plasmonic resonances with a large frequency detuning between the plasmon resonances and PDMS absorbance peaks. Therefore, damping effects of the PDMS substrate on the plasmon resonances is avoided resulting in an enhanced absorption signal in mid-infrared region with larger FOM which is essential for biomolecular identification and isolating its optical response. As a result, the plasmon resonances which are detuned from the absorbance peaks of polymer-based substrate can encompass the molecular vibrational fingerprints for quantitative biomolecule detection and chemical-specific molecular identification.

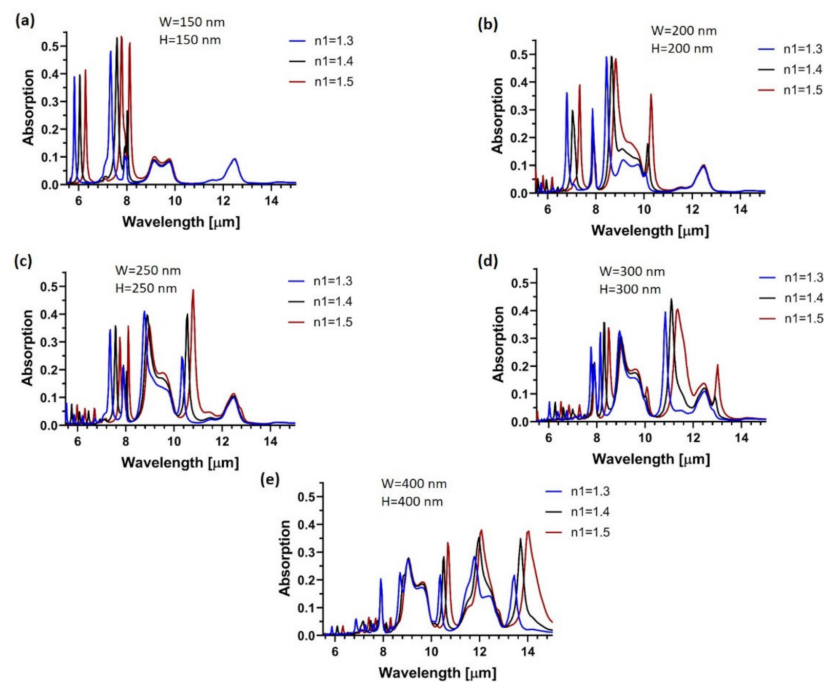


Figure 4. Geometry dependence of the plasmonic resonance shifts in biaxially crumpled graphene structures supported on the PDMS substrate with aspect ratio $W/H = 1$ for (a) $W = H = 150$ nm, (b) $W = H = 200$ nm, (c) $W = H = 250$ nm, (d) $W = H = 300$ nm, and (e) $W = H = 400$ nm. The RI of sample n_1 varies from 1.3 to 1.5. The electronic properties of graphene are set as $E_f = 0.64$ eV and $\mu = 10,000$ cm²/(V·s).

Additionally, we investigated the effects of an insulating substrate on the wavelength shift of plasmonic resonances in biaxially crumpled structures. In this case, silicon oxide (SiO_2) and titanium oxide (TiO_2) were used as substrates to avoid the damping effects of polymer-based substrates on the plasmonic resonances in graphene. Figure 5 shows the wavelength shift of the plasmonic resonances in the transmission spectra of the biaxially crumpled graphene supported on SiO_2 and TiO_2 substrates when the RI of the medium on the graphene surface changed from 1.3 to 1.5. The sensitivity and FOM obtained for crumpled graphene on SiO_2 were 3450 nm/RIU and 44, respectively, which were higher than those for the biaxially crumpled graphene on PS substrate (sensitivity: 3190 nm/RIU and FOM: 24) for the second plasmon mode at a wavelength of approximately 7 μm (Figure 3a). The crumpled graphene on TiO_2 exhibited a sensitivity of 4805 nm/RIU, corresponding to an FOM of 16 for the main plasmonic mode at a wavelength of approximately 9.2 μm . This sensitivity was higher than that achieved in the biaxially crumpled graphene supported on a PDMS substrate. The frequency band in the mid-infrared range of 8.15–9.44 μm , shown in Figure 5a, and frequency bands beyond 11.9 μm , shown in Figure 5b, were attributed to the optical phonons of the SiO_2 and TiO_2 substrates, respectively.

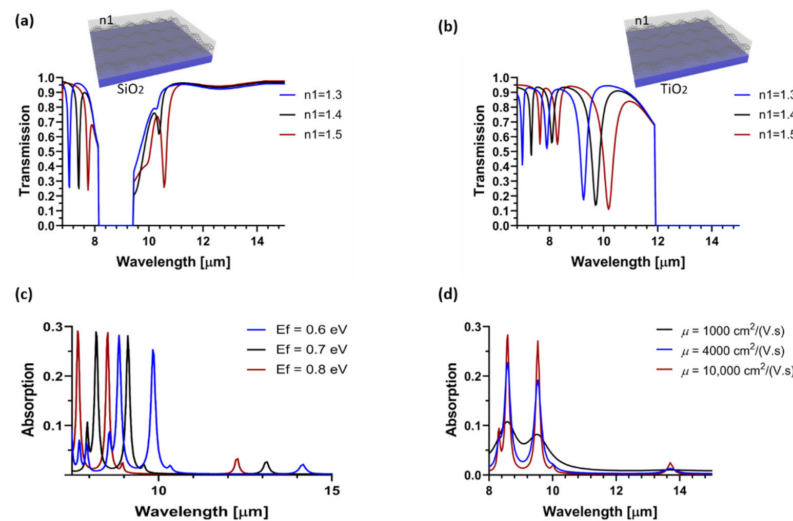


Figure 5. Substrate effect for plasmonic resonance shifts of biaxially crumpled graphene structures supported on (a) SiO_2 , and (b) TiO_2 , when the RI of solution atop the graphene n_1 changes from 1.3 to 1.5, with structural parameters of $W = 250$ nm; $H = 300$ nm; $E_f = 0.64$ eV; and $\mu = 10,000$ $\text{cm}^2/(\text{V}\cdot\text{s})$. (c) Electrical tunability of biaxially crumpled graphene structures by varying E_f from 0.6 to 0.8 eV at $\mu = 10,000$ $\text{cm}^2/(\text{V}\cdot\text{s})$. (d) Optical absorption spectra of biaxially crumpled graphene for various μ values from 1000 to 10,000 $\text{cm}^2/(\text{V}\cdot\text{s})$ at $E_f = 0.64$ eV.

The electrical tunability of plasmonic resonances in the biaxially crumpled graphene could be obtained by varying the Fermi energy level of graphene. As shown in Figure 5c, by increasing E_f from 0.6 to 0.8 eV, the resonance wavelength blue-shifted from approximately 9.8 to 8.5 μm , which represented a larger shift than that achieved in uniaxially crumpled graphene for the same resonance wavelength [28]. Owing to the defects and impurities introduced in graphene on various substrates, the charge-carrier mobility of graphene decreased, thereby resulting in optical losses, and broadening of spectral resonances in the crumpled graphene structures with lower intensity. As shown in Figure 5d, when the mobility decreased from 10,000 to 1000 $\text{cm}^2/(\text{V}\cdot\text{s})$, the absorption intensity decreased from 0.285 to 0.11 for the plasmonic resonance at a wavelength of 8.6 μm . However, the intensity of the plasmon mode at 8.6 μm in the biaxially crumpled graphene was higher than that in the uniaxially crumpled structure with a carrier mobility of 1000 $\text{cm}^2/(\text{V}\cdot\text{s})$ at the same resonance wavelength. This verified the stronger plasmonic resonances of the biaxial structures.

Our proposed biaxially crumpled graphene structure presents a facile fabrication process and strong plasmonic resonances, with broadband spectral tunability from mid-to near-infrared through mechanical reconfiguration of the device. We demonstrated that the biaxially crumpled graphene structure is a promising candidate for use as an RI sensor, with superior sensing performance compared with uniaxially crumpled graphene and conventional graphene-based RI sensors. Compared with flat graphene-based sensors, the 3D formation of the biaxially crumpled graphene structure provided a larger cross-sectional surface area of graphene in contact with biomolecules and solutions, particularly near the concave and convex regions of the wrinkled structure. Whereas strong near-field enhancement and spatial confinement of plasmons could occur locally. This effect, which is the main strength of crumpled graphene structures, appeared more strongly in the biaxially crumpled graphene structure than in the uniaxial structure, thereby demonstrating the enhanced sensitivity of biaxially crumpled graphene structures. Owing to the strong spectral overlap between the large optical absorption of the PDMS substrate and the plasmonic resonances in graphene, the biomolecular response may not be clearly distinguished in the uniaxially crumpled graphene structures on PDMS. In such an interacting system, the SPRs were attenuated and could be overwhelmed by the large optical response of the PDMS layer, which reduced the sensor sensitivity. Distinct plasmon resonances with a higher absorbance intensity and lower FWHM could be observed in biaxially crumpled graphene on the PDMS substrate, which increased the shift in the resonance wavelength in the presence of biomaterials. This is in contrast to the strong coupling regime between the PDMS absorbance and plasmon resonances in uniaxially crumpled graphene. In addition, more plasmon modes could be observed in biaxially crumpled graphene, which were detuned from the destructive PDMS absorbance peaks, thus improving the sensing performance of crumpled graphene-based biosensors.

3. Materials and Methods

To investigate the photoabsorption spectra of the crumpled graphene structures, we performed full-wave optical three-dimensional (3D) simulations using COMSOL Multiphysics (version 5.4) and a radio-frequency module based on the finite element method (FEM) with periodic boundary conditions applied in the respective crumpling directions. At mid-infrared frequencies, where the photon energy is smaller than $2E_f$, the interband transition effect could be ignored and the intraband conductivity (σ_G) of graphene was modeled with a semiclassical Drude model as

$$\sigma_G(\omega) = \frac{2ie^2}{\pi\hbar^2(\omega + i\tau_G^{-1})} k_B T \times \ln\left[2\cosh\left(\frac{E_f}{2k_B T}\right)\right] \quad (1)$$

where k_B is the Boltzmann constant; $T = 300$ K is the temperature; \hbar is the reduced Planck constant; τ_G is the carrier relaxation time, which depends on the carrier mobility μ in graphene as $\tau_{Gr} = \mu E_f / ev_f^2$; and $E_f = \hbar v_f (\pi n)^{1/2}$ is the Fermi energy level, where $v_f = 10^6$ m/s is the Fermi velocity and n is the charge-carrier density in graphene. The permittivity of graphene can be calculated by $\epsilon(\omega) = 2.5 + i\sigma_G / (\epsilon_0 \omega t)$, where t is the thickness of graphene layer, 0.34 nm [32]. In the simulations, the RI of polydimethylsiloxane (PDMS) and polystyrene (PS) substrates, and SiO₂ and TiO₂ substrates were taken from Palik [33].

The momentum mismatching between the free-space electromagnetic wave and plasmon is compensated using the undulated graphene structure which is formed by releasing a pre-strained stretchable polymer substrate after the graphene transferring process. This results in the conversion of incident light into the propagating GPs.

In modeling the structure used as RI sensor, a sensing medium with RI of n_1 is placed on top of the sensor surface for biosensing applications. For flat substrate, the area between the convex of deformed graphene and substrate is filled with air with RI of 1, and the wrinkles are filled with substrate material for undulated structures. The sensing medium was chosen to cover the RI of commonly used biomolecules such as single-stranded DNA, and double-stranded DNA, and proteins. To simulate the real RI sensor, periodic boundary

condition is applied to the unit cell on the corresponding crumpling directions, which creates an array of infinite unit cells. A transverse magnetic (TM) polarized light along the crumpling directions x and y illuminates the structure in the vertical direction (K_0) and periodic port is selected in the z -direction in order to irradiate the whole structure.

Sensitivity (S) and FOM are defined as $S = \Delta\lambda / \Delta n$ and $FOM = S(nm \times RIU^{-1}) / FWHM$, respectively, where $\Delta\lambda$ is the amount of spectral shift in the resonance wavelength (λ) with respect to the RI variations (Δn) of the sample medium, and FWHM is the full width at half maximum of the resonance peak.

4. Conclusions

In conclusion, we presented a new RI sensor based on plasmonic resonances in biaxially crumpled graphene structures for operation in the mid-IR region. The novel 3D biaxially crumpled graphene structure enables strong biomolecule–graphene plasmon interaction, which enhances sensitivity. Numerical simulations demonstrated sensitivities as high as 2650 nm/RIU (4990 nm/RIU), corresponding to FOM values of 16(20) for biaxially crumpled graphene on PDMS(PS). Through the mechanical reconfiguration of crumpled graphene structures, sensor sensitivity could be tuned over a broad spectral range in the mid-infrared region. The biaxially crumpled graphene structures exhibited superior sensing performance compared with the uniaxial structures. Furthermore, the use of an oxide layer as a substrate can avoid the damping effect of polymer substrates, thereby enhancing the sensing performance of crumpled graphene structures. The proposed RI sensor exhibited a high sensitivity of 4810 nm/RIU and FOM of 16 for crumpled graphene on the TiO_2 substrate. The highly sensitive RI sensor, along with its broadband tunability and facile fabrication process, holds excellent promise for potential applications in the development of high-performance biosensing platforms in the mid-infrared region. These optical sensors convert the analyte information or the biochemical interactions into a quantifiable signal by investigating the changes in the optical responses of the sensors, such as phase, intensity, and frequency, revealed because of the presence of the biological samples. These configurations offer considerable promise for human health-monitoring application since the cancerization of cells and the invasion of viruses are often accompanied by changes in refractive index statistically. They are also widely used for monitoring surface-binding event, determining the amount of biomolecules and their material purity and concentration, detection of analyte layers, and study of antigen–antibody interaction dynamics. With their highly sensitivity, selectivity, rapid, small footprint, these platforms contribute to advances in next-generation medicines such as personalized medicine and ultrasensitive point-of-care detection of diseases biomarkers in healthcare.

Author Contributions: Conceptualization, V.F.; methodology, V.F.; software, V.F., M.H. and N.H.b.N.Z.; validation, M.T.H.; formal analysis, V.F., M.T.H. and M.H.; investigation, V.F. and M.T.H.; resources, M.T.H.; writing—original draft preparation, V.F. and M.T.H.; writing—review and editing, V.F., M.T.H., M.H. and N.H.b.N.Z.; visualization, V.F., M.T.H. and M.H.; supervision, M.T.H.; project administration, M.T.H. and V.F.; funding acquisition, M.T.H. All authors have read and agreed to the published version of the manuscript.

Funding: This work was supported by the Gachon University research fund of 2020 (GCU-202008430008).

Data Availability Statement: All data in this work will be made available from the corresponding author upon reasonable request.

Conflicts of Interest: The authors declare no conflict of interest.

References

1. Linman, M.J.; Sugerman, K.; Cheng, Q. Detection of low levels of *Escherichia coli* in fresh spinach by surface plasmon resonance spectroscopy with a TMB-based enzymatic signal enhancement method. *Sens. Actuators B Chem.* **2010**, *145*, 613–619. [[CrossRef](#)]
2. Szunerits, S.; Boukherroub, R. Sensing using localised surface plasmon resonance sensors. *Chem. Commun.* **2012**, *48*, 8999–9010. [[CrossRef](#)]

3. Laing, S.; Jamieson, L.E.; Faulds, K.; Graham, D. Surface-enhanced Raman spectroscopy for in vivo biosensing. *Nat. Rev. Chem.* **2017**, *1*, 60. [[CrossRef](#)]
4. Homola, J. Surface plasmon resonance sensors for detection of chemical and biological species. *Chem. Rev.* **2008**, *108*, 462–493. [[CrossRef](#)] [[PubMed](#)]
5. Abdulhalim, I.; Zourob, M.; Lakhtakia, A. Surface plasmon resonance for biosensing: A mini-review. *Electromagnetics* **2008**, *28*, 214–242. [[CrossRef](#)]
6. Narsaiah, K.; Jha, S.N.; Bhardwaj, R.; Sharma, R.; Kumar, R. Optical biosensors for food quality and safety assurance—A review. *J. Food Sci. Technol.* **2012**, *49*, 383–406. [[CrossRef](#)] [[PubMed](#)]
7. Saha, N.; Brunetti, G.; Kumar, A.; Armenise, M.N.; Ciminelli, C. Highly sensitive refractive index sensor based on polymer bragg grating: A case study on extracellular vesicles detection. *Biosensors* **2022**, *12*, 415. [[CrossRef](#)] [[PubMed](#)]
8. Im, H.; Shao, H.; Park, Y.I.; Peterson, V.M.; Castro, C.M.; Weissleder, R.; Lee, H. Label-free detection and molecular profiling of exosomes with a nano-plasmonic sensor. *Nat. Biotechnol.* **2014**, *32*, 490–495. [[CrossRef](#)] [[PubMed](#)]
9. Park, J.; Park, J.S.; Huang, C.-H.; Jo, A.; Cook, K.; Wang, R.; Lin, H.-Y.; Van Deun, J.; Li, H.; Min, J.; et al. An integrated magneto-electrochemical device for the rapid profiling of tumour extracellular vesicles from blood plasma. *Nat. Biomed. Eng.* **2021**, *5*, 678–689. [[CrossRef](#)]
10. Homola, J. Present and future of surface plasmon resonance biosensors. *Anal. Bioanal. Chem.* **2003**, *377*, 528–539. [[CrossRef](#)] [[PubMed](#)]
11. Chen, X.; Wang, Y.; Xiang, Y.; Jiang, G.; Wang, L.; Bao, Q.; Zhang, H.; Liu, Y.; Wen, S.; Fan, D. A broadband optical modulator based on a graphene hybrid plasmonic waveguide. *J. Lightwave Technol.* **2016**, *34*, 4948–4953. [[CrossRef](#)]
12. Ju, L.; Geng, B.; Horng, J.; Girit, C.; Martin, M.; Hao, Z.; Bechtel, H.A.; Liang, X.; Zettl, A.; Shen, Y.R.; et al. Graphene plasmonics for tunable terahertz metamaterials. *Nat. Nanotechnol.* **2011**, *6*, 630–634. [[CrossRef](#)] [[PubMed](#)]
13. Zhang, Y.; Li, T.; Zeng, B.; Zhang, H.; Lv, H.; Huang, X.; Zhang, W.; Azad, A.K. A graphene based tunable terahertz sensor with double Fano resonances. *Nanoscale* **2015**, *7*, 12682–12688. [[CrossRef](#)] [[PubMed](#)]
14. Du, Z.; Hu, B.; Cyril, P.; Liu, J.; Wang, Y. High sensitivity plasmonic sensor using hybrid structure of graphene stripe combined with gold gap-ring. *Mater. Res. Express* **2017**, *4*, 105013. [[CrossRef](#)]
15. Li, H.J.; Wang, L.L.; Sun, B.; Huang, Z.R.; Zhai, X. Controlling mid infrared surface plasmon polaritons in the parallel graphene pair. *Appl. Phys. Express* **2014**, *7*, 125101. [[CrossRef](#)]
16. Faramarzi, V.; Ahmadi, V.; Ghane Golmohamadi, F.; Fotouhi, B. A biosensor based on plasmonic wave excitation with diffractive grating structure. *Sci. Iran.* **2017**, *24*, 3441–3447. [[CrossRef](#)]
17. Cen, C.; Lin, H.; Huang, J.; Liang, C.; Chen, X.; Tang, Y.; Yi, Z.; Ye, X.; Liu, J.; Yi, Y.; et al. A tunable plasmonic refractive index sensor with nanoring-strip graphene arrays. *Sensors* **2018**, *18*, 4489. [[CrossRef](#)]
18. Wenger, T.; Viola, G.; Kinaret, J.; Fogelström, M.; Tassin, P. High sensitivity plasmonic refractive index sensing using graphene. *2D Mater.* **2017**, *4*, 025103. [[CrossRef](#)]
19. Faramarzi, V.; Ahmadi, V.; Heidari, M.; Fotouhi, B.; Hwang, M.T. Interband plasmon-enhanced optical absorption of dna nucleobases through the graphene nanopore. *Opt. Lett.* **2022**, *47*, 194–197. [[CrossRef](#)]
20. Fotouhi, B.; Ahmadi, V.; Faramarzi, V. Nano-plasmonic-based structures for dna sequencing. *Opt. Lett.* **2016**, *41*, 4229–4232. [[CrossRef](#)]
21. Fotouhi, B.; Ahmadi, V.; Abasifard, M.; Faramarzi, V. Petahertz frequency plasmons in graphene nanopore and their application to nanoparticle sensing. *Sci. Iran.* **2017**, *24*, 1669–1677. [[CrossRef](#)]
22. Rodrigo, D.; Limaj, O.; Janner, D.; Etezadi, D.; García de Abajo, F.J.; Pruneri, V.; Altug, H. Mid-infrared plasmonic biosensing with graphene. *Science* **2015**, *349*, 165–168. [[CrossRef](#)] [[PubMed](#)]
23. Zhang, J.; Zhang, L.; Xu, W. Surface plasmon polaritons: Physics and applications. *J. Phys. D Appl. Phys.* **2012**, *45*, 113001. [[CrossRef](#)]
24. Kang, P.; Kim, K.H.; Park, H.G.; Nam, S. Mechanically reconfigurable architected graphene for tunable plasmonic resonances. *Light. Sci. Appl.* **2018**, *7*, 17. [[CrossRef](#)] [[PubMed](#)]
25. Hwang, M.T.; Heiranian, M.; Kim, Y.; You, S.; Leem, J.; Taqieddin, A.; Faramarzi, V.; Jing, Y.; Park, I.; van der Zande, A.M.; et al. Ultrasensitive detection of nucleic acids using deformed graphene channel field effect biosensors. *Nat. Commun.* **2020**, *11*, 1543. [[CrossRef](#)]
26. Ganguli, A.; Faramarzi, V.; Mostafa, A.; Hwang, M.T.; You, S.; Bashir, R. High sensitivity graphene field effect transistor-based detection of dna amplification. *Adv. Funct. Mater.* **2020**, *30*, 2001031. [[CrossRef](#)]
27. Hwang, M.T.; Park, I.; Heiranian, M.; Taqieddin, A.; You, S.; Faramarzi, V.; Pak, A.A.; van der Zande, A.M.; Aluru, N.R.; Bashir, R. Ultrasensitive detection of dopamine, il-6 and sars-cov-2 proteins on crumpled graphene fet biosensor. *Adv. Mater. Technol.* **2021**, *6*, 2100712. [[CrossRef](#)]
28. Faramarzi, V.; Ahmadi, V.; Hwang, M.T.; Snapp, P. Highly sensitive crumpled 2d material-based plasmonic biosensors. *Biomed. Opt. Express* **2021**, *12*, 4544–4559. [[CrossRef](#)]
29. Tong, K.; Wang, Y.; Wang, F.; Sun, J.; Wu, X. Surface plasmon resonance biosensor based on graphene and grating excitation. *Appl. Opt.* **2019**, *58*, 1824–1829. [[CrossRef](#)]
30. Gong, S.; Xiao, B.; Xiao, L.; Tong, S.; Xiao, S.; Wang, X. Hybridization-induced dual-band tunable graphene metamaterials for sensing. *Opt. Mater. Express* **2019**, *9*, 35–43. [[CrossRef](#)]

-
31. Wu, D.; Tian, J.; Li, L.; Yang, R. Plasmon induced transparency and refractive index sensing in a new type of graphene-based plasmonic waveguide. *Opt. Commun.* **2018**, *412*, 41–48. [[CrossRef](#)]
 32. Gao, W.; Shu, J.; Qiu, C.; Xu, Q. Excitation of plasmonic waves in graphene by guided-mode resonances. *ACS Nano* **2012**, *6*, 7806–7813. [[CrossRef](#)] [[PubMed](#)]
 33. Palik, E.D. *Handbook of Optical Constants of Solids*, 1st ed.; Academic Press: San Diego, CA, USA, 1998; p. 3187.